



Protein Immobilization onto Silicon Nanowires via Electrografting of Hexynoic Acid

Z. R. Scheibal,^a W. Xu,^{a,*} J. F. Audiffred,^b J. E. Henry,^a and J. C. Flake^{a,**,z}

^aGordon and Mary Cain Department of Chemical Engineering and ^bDepartment of Biological and Agricultural Engineering, Louisiana State University, Baton Rouge, Louisiana 70803, USA

Electrografting provides a method for the direct (Si–C) covalent functionalization of silicon surfaces. In this work, cathodic electrografting of hexynoic acid to silicon nanowire surfaces and subsequent immobilization of bovine serum albumin (BSA) is demonstrated. Hexynoic acid was cathodically electrografted to dense arrays of silicon nanowires approximately 50–100 nm in diameter and 10 μm in length. Protein immobilization was achieved via amidization reactions with carboxylic moieties of electrografted hexynoic acids. Results include chronoamperometric data from the electrografting process and verification of attachment using attenuated total reflectance Fourier transform infrared spectroscopy (FTIR) of electrografted hexynoic acid and immobilized BSA. In addition to FTIR analysis, covalently immobilized BSA was verified using fluorescence microscopy and solution-phase fluorescence.

© 2008 The Electrochemical Society. [DOI: 10.1149/1.2937178] All rights reserved.

Manuscript submitted January 3, 2008; revised manuscript received May 6, 2008. Available electronically June 5, 2008.

In recent years there has been significant interest in the modification of nanoscale silicon surfaces for bioelectronic applications.^{1–3} In comparison with immobilization techniques such as adsorption or membrane attachment, covalent bonding produces the highest surface loading and lowest protein loss due to desorption.⁴ Typically, covalent immobilization of proteins onto silicon surfaces involves the functionalization of silicon dioxide or silica surfaces using silane coupling reactions. Silane coupling reactions are capable of providing high surface loading (10^{12} molecules/cm²), and the oxide interface typically shows good thermal stability.⁴ In many sensor applications, however, the oxide layer used to covalently attach proteins to the surface includes high levels of defects and the physical separation caused by the oxide layer diminishes the optical or electrical signals needed for detection.²

As an alternative to silane coupling reactions, several works have considered direct (Si–C) bonding of organic molecules to silicon hydride surfaces.^{5–12} Silicon surfaces may be functionalized via cycloaddition reactions¹² or hydrosilylation of hydride-terminated surfaces with alkenes and alkynes via radical initiators, thermal activation, or UV exposure.⁵ Work by Sieval et al. has shown thermally initiated reactions of silicon hydride surfaces with ester-functionalized alkenes.⁶ Based on IR and X-ray reflectometry results, the authors show unprotected esters result in monolayers with relatively greater disorder compared to protected esters. Bunimovich et al. has also shown UV-initiated hydrosilylation reactions of silicon hydride surfaces with protected hydroquinones.² While these methods are effective, the processes require relatively longer reaction times (~ 2 h for thermal and UV-initiated hydrosilylation) and may require a deprotection step to create well-ordered monolayers. Work by Buriak et al.^{5,7–10} and Stewart et al.¹¹ has shown it is possible to create Si–C bonds (including nanoscale patterning of silicon surfaces) by cathodic electrografting of various alkynes and alkenes, including straight chain and aryl- or bromo-functional alkynes, to hydride-terminated silicon.

More specifically, functionalization of silicon nanowire surfaces has been demonstrated using lithographically defined silicon nanowires, vapor-liquid-solid grown silicon nanowires, and via gold-on-silicon nanowires defined by scanning probe lithography; however, most of these methods involve silanes and an intermediate oxide layer.^{1,3,13} Work by Sheu et al. demonstrated the ability to detect enzymes (bound to gold nanoparticles on amino-functional silanes) with silicon nanowires formed by scanning probe lithography.¹³ Recently, Stern et al. described lithographically defined silicon nanowire field effect transistor biosensors with extraordinary sensitivity,

demonstrating detection of antibodies at the femtomolar level.¹ Here, we demonstrate a method to immobilize proteins directly onto silicon nanowires (formed by electrochemical etching of single-crystal silicon wafers) via cathodic electrografting of a carboxyl functional alkyne (hexynoic acid). A prime advantage of this technique is the ability to efficiently bind biomolecules in close proximity to silicon surfaces with direct Si–C bonds for biosensor applications.

Direct bonding is expected to improve electrical sensitivity of semiconductor sensors due to the increased proximity of the target and sensor surface, reduced defect density, and reduced roughness associated with silicon dioxide surfaces.^{2,14} Silicon nanowires formed by VLS growth and lithography have been directly functionalized (with protected amines) via UV-initiated hydrosilylation for applications as DNA sensors or alkali metal ion sensors.^{15,16} As described in the work by Bunimovich et al., the sensitivity of silicon nanowire DNA sensors without oxides (also functionalized via UV-initiated hydrosilylation) increased limits of detection by more than 2 orders of magnitude.¹⁴ In addition, the absence of an oxide layer reduces electrostatic screening effects (Debye screening), further increasing sensitivity to target molecules at silicon nanowire surfaces.^{14,17} The work described here provides a fast method for direct bonding and functionalization of silicon nanowires. In this case, the method provides a carboxyl-functionalized surface and does not require any intermediate binding agents or deprotection steps.

Experimental

Prime-grade p-type 100 mm silicon wafers (100) with a resistivity range of 1–5 Ω cm (Montco, Spring City, PA) were used in all electrografting experiments. Silicon nanowires were created using cleaved samples from single-crystal wafers in an electroless process with HF (Aldrich, USA).¹⁸ A supporting electrolyte, 0.6 M tetrabutylammonium tetrafluoroborate (TBABF₄), was added to hexynoic acid (2-hexynoic acid 97%, Aldrich) in electrografting experiments. Silicon samples were cleaned with an aqueous solution of 0.01 M buffered HF followed by cathodic electrografting in an electrochemical cell with a Pt foil counter electrode. Electrografting was performed under constant cross-cell potentials where the silicon substrate was used as the working electrode. Potentiostatic experiments were performed using a PAR 263A potentiostat (Oak Ridge, TN). Fourier transform infrared (FTIR) analysis of grafted surfaces was performed after electrografting and cleaning on a Thermo-Nicolet 380 (Waltham, MA) using a multibounce attenuated total reflection (ATR) attachment with a zinc selenide crystal. Amidization reactions of hexynoic acid and bovine serum albumin (BSA, concentration ~ 20 g/L) were carried out in a 0.2 M 2-(*N*-morpholino)methanesulfonic acid conjugation buffer at a pH 5. 1-Ethyl-3-[3-dimethylaminopropyl] carbodimide hydrochloride

* Electrochemical Society Student Member.

** Electrochemical Society Active Member.

^z E-mail: johnflake@lsu.edu

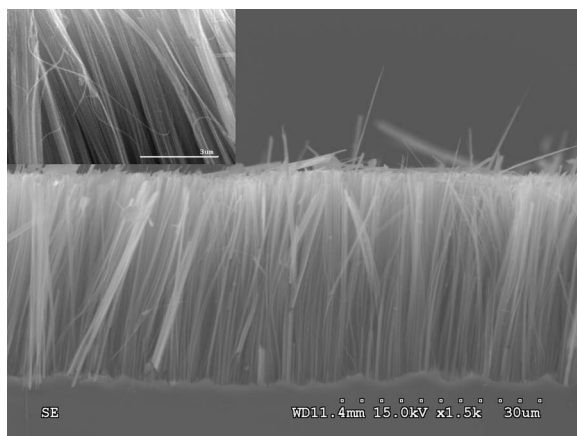


Figure 1. Scanning electron microscope cross section showing freestanding silicon nanowires etched from a Si(100) wafer. Inset image shows magnified view of nanowires.

(EDC) 20 g/L from Pierce Biotechnology (Rockford, IL) was used as a catalyst in amidization reactions. Electrografted silicon samples remained in the BSA/EDC solution for 12 h followed by seven (30 s) clean cycles using deionized (DI) water and nitrogen drying. Surface binding was verified using single-bounce FTIR and fluorescent labeling. Fluorescent protein labeling was performed using fluorescein isothiocyanate (FITC) from Invitrogen (Carlsbad, CA). Following fluorescent labeling, nanowires were separated from the parent wafer in DI water using ultrasonic agitation. Nanowires were centrifuged (19,000 rpm, 10 min) and the solution was removed. Fresh phosphate buffer solution was added to centrifuged nanowires followed by agitation to suspend. Quantitative fluorescence analysis was performed using an Olis DSM 420 CD fluorimeter (Bogart, GA). In addition to solution-phase fluorometrics, separated nanowires were imaged using bright-field phase contrast and fluorescence microscopy at 40 \times magnification. Images were acquired with an inverted Eclipse TS100 Nikon fluorescence microscope equipped with an FITC filter set and a CoolSnapFX camera (Photometrics, Tucson, AZ). Fluorescent images were acquired for a 10 s exposure with 2 \times 2 binning. The bright-field and FITC images were processed using MetaVue software (Universal Imaging Corp., West Chester, PA).

Results and Discussion

As shown in Fig. 1, dense arrays (approximately 1–10 billion nanowires per cm²) of silicon nanowires with diameters <100 nm and near 10 μ m in length were created in a subtractive process from a (100) p-type Si wafer. Silicon surfaces with nanowires (approximately 10 μ m in length) appear dark and nonreflective after electrochemical etching for 30 min and rinsing with dilute HNO₃. Following etching and cleaning with dilute HNO₃ and dilute HF, nanowire substrates were anodically biased in an electrochemical cell containing hexynoic acid with 0.6 M TBABF₄.

In chronoamperometric experiments, cross-cell potential was maintained at 9.0 V and current was monitored for 60 s. Shown in Fig. 2 are current densities as a function of electrografting time normalized to the steady-state current density at 60 s. The normalized current density shows an initial peak followed by an exponential decrease with time. This behavior suggests low coulombic efficiencies toward electrografting. After 60 s of electrografting, current densities remained relatively constant (<5% change over 5 min); however, the steady-state current density ranged from 100 to 500 μ A/cm depending on experimental conditions. This range in current density appears to be associated with other reactions with trace impurities or the supporting electrolyte and does not appear to lead to the formation of thicker (multilayer) electrografted films. Figure 5 shows relatively little difference between normalized current density as a function of time for unetched and etched (nanowire) silicon surfaces. Similar current–voltage behavior is expected as the increased area due to nanowire formation is less than 0.1% greater than the unetched samples. Based on this self-passivating behavior and surface wetting, formation of an electrografted hexynoic film appears to occur within the first 10–30 s of applied potential. Following electrografting experiments, samples were removed from the electrochemical cell and cleaned with acetone, isopropyl alcohol, and several DI water rinses followed by nitrogen drying.

As shown in Fig. 3, multibounce FTIR analysis confirms the attachment of hexynoic acid to silicon nanowire surfaces. FTIR spectra of neat hexynoic acid shows characteristic peaks at 1699 cm⁻¹ for carboxylic C=O stretching and 1148 cm⁻¹ for the O–H stretch. There are peaks for methyl stretching that appear at 2960 and 2870 cm⁻¹. As with the neat hexynoic spectra, silicon nanowire surfaces with electrografted hexynoic acid also show characteristic carboxylic peaks at 1699 cm⁻¹ for carboxylic C=O stretching and 1150 cm⁻¹ from the carboxylic O–H stretch. The

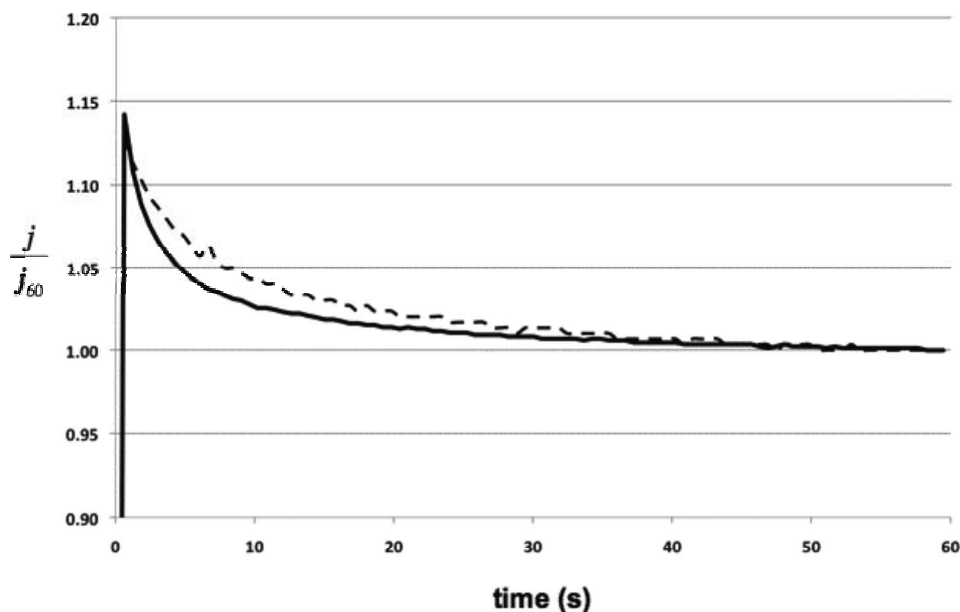


Figure 2. Chronoamperogram showing normalized current density (j/j_{60}) for cathodic electrografting of hexynoic acid onto silicon (solid line) and onto silicon nanowires (dashed line).

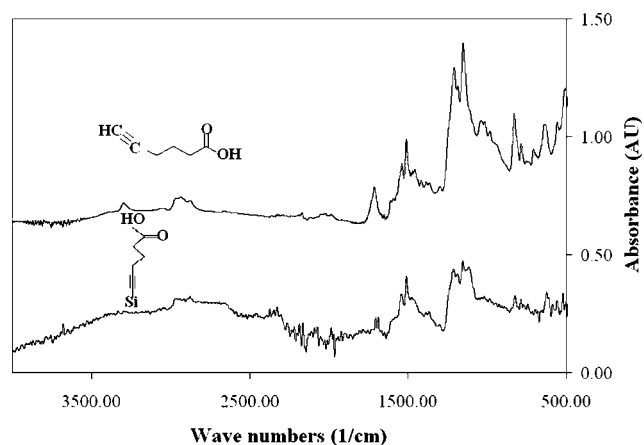


Figure 3. ATR FTIR spectra showing neat hexynoic acid (top) and surface-bound hexynoic acid (electrografted to a silicon nanowire surface).

slight shifts ($\sim 2 \text{ cm}^{-1}$) for the carboxylic C=O and O-H stretching are repeatable and appear to be due to the nature of bound hexynoic acid. In addition to the characteristic carboxyl peaks, the electrografted hexynoic spectra also shows excellent matching with the methyl stretching 2955 and 2872 cm^{-1} and scissoring 1505 cm^{-1} . The peak at 3290 cm^{-1} for the triple carbon bond is not observed, consistent with previous work.⁷

Amidization reactions of the electrografted carboxyl moieties bound to the silicon nanowire surface were used to immobilize BSA proteins. Nanowires were exposed to BSA and EDC solutions for 12 h. Shown in Fig. 4 are single-bounce ATR (diamond crystal) spectra for pure BSA and immobilized BSA onto a silicon surface. The single-bounce method was used in this case due to the relatively small sample size of the nanowire substrate. Peaks at 1636 and 1515 cm^{-1} for the BSA alone and at 1610 and 1505 cm^{-1} for the electrografted BSA are associated with primary amides. The immobilized BSA spectra are not affected by multiple rinses with DI water or wiping of the surface with a Textwipe cloth.

Immobilization was further verified using solution-phase fluorescence analysis of nanowires. Nanowires with immobilized BSA were separated from the substrate in an aqueous solution by ultrasonic agitation followed by centrifuging, rinsing, and fluorescent labeling with FITC. All unbound fluorescent dye was removed by three iterations of centrifuging and rinsing. Following resuspension, transmission fluorescence analysis was performed in an Olis monochromator using a 492 nm light source. As shown in Fig. 5, fluores-

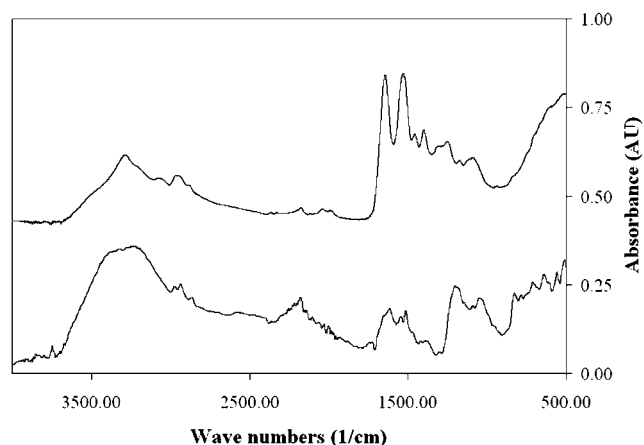


Figure 4. FTIR spectra showing BSA (top) and immobilized BSA onto a silicon nanowire substrate.

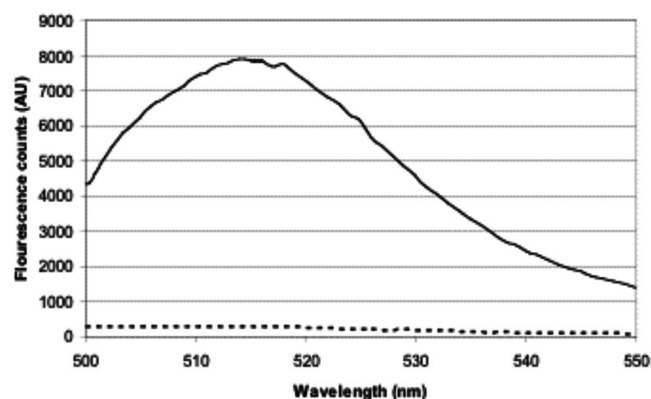


Figure 5. Photoemission scan of nanowires in solution using an Olis DSM 20 CD fluorimeter. Solid line: fluorescently labeled nanowires in solution, dotted line: control.

cence and BSA immobilization is only associated with electrografted and BSA-immobilized nanowire solutions. A control experiment with solutions of nanowires that were not electrografted with hexynoic acid but treated in FITC for 12 h does not show significant fluorescence. Additional control experiments including silicon nanowires electrografted with hexynoic and treated in FITC for 12 h (not exposed to BSA) and nonelectrografted nanowires treated in BSA for 12 h followed by FITC labeling also showed no fluorescence.

To further confirm the fluorescence originates from the surface of nanowires rather than the carrier solution, nanowires with FITC-labeled and immobilized BSA were examined using fluorescence microscopy. Nanowire samples were DI water rinsed and nitrogen dried seven times then separated from the parent wafer by ultrasonic agitation followed by a series ($3\times$) of centrifugation, washes, and resuspension in DI water. A droplet of the aqueous solution with nanowires was deposited onto a microscope slide for fluorescence microscopy. As shown in Fig. 6, results show a clear association of fluorescence with the nanowires (no background fluorescence) and the lack of fluorescence in the control groups (both nonelectrografted and nonimmobilized control samples).

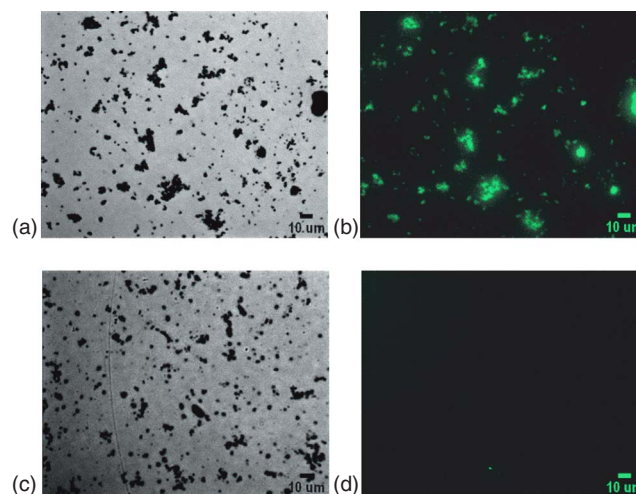


Figure 6. (Color online) Optical and fluorescence images of aqueous solution droplets containing nanowires: (a) optical image of nanowires bonded with BSA treated with FITC, (b) fluorescence image of (a), (c) optical image of nonelectrografted nanowires treated with FITC, and (d) fluorescence image of (c).

Conclusions

In this work we have demonstrated a technique to immobilize proteins directly onto dense arrays of silicon nanowire surfaces. Silicon nanowire surfaces were cathodically electrografted with hexynoic acid in 60 s and direct protein immobilization (without oxide intermediates) was demonstrated. Electrografting of hexynoic acid was verified using ATR FTIR. Immobilization of BSA onto nanowire surfaces was also verified using FTIR of silicon nanowire surfaces, solution-phase fluorescence, and microfluorescence. This method demonstrates an efficient route to surface functionalization and allows immobilization of amino-functional proteins in close proximity to the silicon surface without any intermediate binding or deprotection steps.

Louisiana State University assisted in meeting the publication costs of this article.

References

1. E. Stern, J. F. Klemic, D. A. Routenberg, P. N. Wyrembak, D. B. Turner-Evans, A. D. Hamilton, D. A. Lavan, T. M. Fahmy, and M. A. Reed, *Nature*, **445**, 519 (2007).
2. Y. L. Bunimovich, G. Ge, K. C. Beverly, R. S. Ries, L. Hood, and J. R. Heath, *Langmuir*, **20**, 10630 (2004).
3. I. Park, Z. Li, A. P. Pisano, and R. S. Williams, *Nano Lett.*, **7**, 3106 (2007).
4. R. A. Williams and H. W. Blanch, *Biosens. Bioelectron.*, **9**, 159 (1994).
5. J. M. Buriak, *Chem. Rev. (Washington, D.C.)*, **102**, 1271 (2002).
6. A. B. Sieval, A. L. Demirel, J. W. M. Nissink, M. R. Linford, J. H. van der Maas, W. H. de Jeu, H. Zuilhof, and E. J. R. Sudholter, *Langmuir*, **14**, 1759 (1998).
7. E. G. Robins, M. P. Stewart, and J. M. Buriak, *Chem. Commun. (Cambridge)*, **1999**, 2479.
8. P. T. Hurley, A. E. Ribbe, and J. M. Buriak, *J. Am. Chem. Soc.*, **125**, 11334 (2003).
9. M. P. Stewart, E. G. Robins, T. W. Geders, M. J. Allen, H. Cheul Choi, and J. M. Buriak, *Phys. Status Solidi A*, **182**, 109 (2000).
10. D. Wang and J. M. Buriak, *Surf. Sci.*, **590**, 154 (2005).
11. M. P. Stewart, F. Maya, D. V. Kosynkin, S. M. Dirk, J. J. Stapleton, C. L. McGuiness, D. L. Allara, and J. M. Tour, *J. Am. Chem. Soc.*, **126**, 370 (2004).
12. F. Tao, Z. H. Wang, M. H. Qiao, Q. Liu, W. S. Sim, and G. Q. Xu, *J. Chem. Phys.*, **115**, 8563 (2001).
13. J. T. Sheu, C. C. Chen, P. C. Huang, and M. L. Hsu, *Microelectron. Eng.*, **78-79**, 294 (2005).
14. Y. L. Bunimovich, Y. S. Shin, W. S. Yeo, M. Amori, G. Kwong, and J. R. Heath, *J. Am. Chem. Soc.*, **128**, 16323 (2006).
15. J. A. Streifer, H. Kim, B. M. Nichols, and R. J. Hamers, *Nanotechnology*, **16**, 1868 (2005).
16. G.-J. Zhang, A. Agarwal, K. D. Buddharaju, N. Singh, and Z. Gao, *Appl. Phys. Lett.*, **90**, 233903 (2007).
17. S. Q. Lud, M. G. Nikolaidis, I. Haase, M. Fischer, and A. R. Bausch, *ChemPhysChem*, **7**, 379 (2006).
18. T. Qiu, X. L. Wu, Y. F. Mei, G. J. Wan, P. K. Chu, and G. G. Siu, *J. Cryst. Growth*, **277**, 143 (2005).